ACS OMEGA

Open Access

http://pubs.acs.org/journal/acsodf

Article

Solubility and Thermodynamic Parameters of H_2S/CH_4 in Ionic Liquids Determined by ^1H NMR

Jeannette Zárraga,* Mariana Zapata, Darmenia Ibarra, Darlin Duarte, Ángel Morillo, Ligia Llovera, Eduardo Gonzalez, Victor Ferrer, and Juan Chirinos*

Cite This: *ACS Omega* 2024, 9, 3588−3595

Read Online

ACCESS | Metrics & More | Article Recommendations | Supporting Information

ABSTRACT: Natural gas remains an important global source of energy. Usually, sour gas from the well or refinery stream contains H_2S among other contaminants that should be removed to fulfill permissible standards of use. Despite the use of different gas−liquid sour gas upgrading technologies, ionic liquids (ILs) have been recognized as promising materials to remove H_2S from sour gas. However, data concerned with thermodynamic solution functions of H_2S in ILs have scarcely been reported in the literature. In this work, solution ^1H NMR spectroscopy was employed for quantifying H_2S soluble in [BMIM][Cl] and for gaining a better understanding of the H_2S−IL interaction. Experiments were carried out in a Young-Tap NMR tube containing a saturated solution of H_2S/CH_4/[BMIM][Cl] and recording spectra from 298 to 333 K. The thermodynamic solution functions, determined from the Van't Hoff equation, showed that solubility of the H_2S in the [BMIM][Cl] is an exothermic gas−liquid physisorption process ($\Delta_{sol}H° = -66.13$ kJmol^{-1}) with a negative entropy change ($\Delta_{sol}S° = -168.19$ JK^{-1} mol^{-1}). ^1H NMR spectra of the H_2S/[BMIM][Cl] solution show a feature of strong solute−solvent interactions. However, solubility enthalpy is a fifth of the H−S bond energy value. Results from ^1H NMR spectroscopy also agree with those from the bench dynamic experiments.

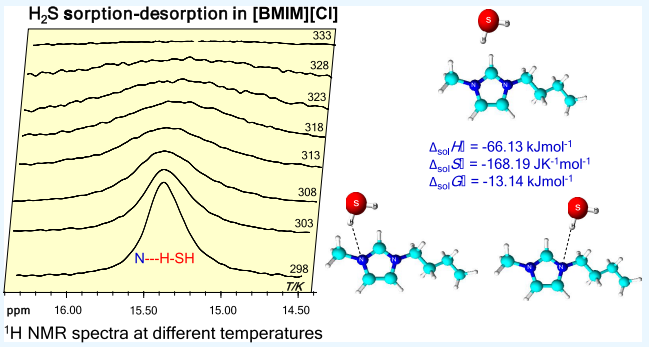

^1H NMR spectra at different temperatures

1. INTRODUCTION

Hydrogen sulfide present in natural and refinery sour gas streams must be removed to avoid critical damage to the industrial platform, due to their high corrosivity, and to fulfill standard requirements of safety and environment.[1−3] Chemical absorption in amine solutions is the most widespread industrial process used for the removal of CO_2 and H_2S from sour gas. In the gas−liquid absorption process, sour gases are contacted with an amine solution to achieve a selective and intensive mass transfer of the CO_2 and/or H_2S, contained in the natural gas, to the inflow liquid. As the amine solution saturates with acid gas, it is regenerated by taking off the H_2S or CO_2 in a second and parallel process.[4,5] Amine solution is further continually reused. The gas absorption step requires low temperature and high pressure, while the desorption step requires high temperature and low pressure. Usually, an amine solution of monoethanolamine (MEA), diethanolamine (DEA), diisopropylamine, methyldiethanolamine, or a mixture of them is employed.[5−9]

Although the amine technology is effective for sour gas sweetening, the chemical nature of the amine used as a sorbent accounts for several disadvantages. First, the lower the chemical stability, the amines undergo chemical degradation to form corrosive byproducts. Second, their high volatility results in an important loss of mass of amine during the regeneration step, which is carried out at a high temperature, and contacting sour gas with the amine solution results in the transfer of water into the sweet-gas stream. Nevertheless, this technology is energy cost-extensive due to the amines are not regenerated under mild conditions.[2,5,8,9]

Since ionic liquids (ILs) were proposed as an eco-friendly alternative solvent for many industrial processes used in sweetening technology of sour-natural gas,[10−13] they have raised a lot of expectations due to their exceptional characteristics of no volatility, negligible vapor pressure, and high chemical, and thermal stability. Furthermore, all the physicochemical properties are tuned by a judicious combination of cations and anions.[14]

To design sour gas sweetening processes based on the IL, knowledge of apparent solution standard enthalpy, entropy, and Gibbs free energy ($\Delta_{sol}H°$, $\Delta_{sol}S°$, and $\Delta_{sol}G°$) and of acid

Received: September 30, 2023
Revised: December 11, 2023
Accepted: December 14, 2023
Published: January 8, 2024

gases in the selected liquids is required. These parameters may be readily estimated from solubility data at different temperatures using the Van't Hoff equation.[15]

Usually, experimental approaches for determining the solubility of H_2S in different liquids are based on gravimetric, electrochemical, semiconducting, thermal, spectroscopic, and optical sensors. Nevertheless, ^{1}H NMR spectroscopy has been used for qualitative and quantitative analysis of H_2S in ILs. For instance, ^{1}H NMR has been recognized as a useful and nonambiguous tool for (i) quantifying sulfide e-trapping efficiency of 1,3,5-tris(2-hydroxyethyl)-1,3,5-triazinane,[16] (ii) demonstrating the mechanistic aspect of the capture of H_2S gas in an organic superbase, DBU, through ionic solid formation (the formation of salt was also confirmed by ^{13}C NMR analysis),[11] and (iii) monitoring the formation of TrtSH from the reaction between TrtSSH and different nucleophiles,[17] among others.

While solubility and diffusivity of H_2S have been widely studied using different experimental and theoretical approaches,[18−21] to the best of our knowledge, scarcely data for solution thermodynamic parameters in ILs have been reported. In this work, we estimate the solution thermodynamic parameter of H_2S of a CH_4/H_2S gas mixture in [BMIM][Cl], using ^{1}H NMR spectroscopy solution techniques. To achieve that, in situ experiments at different temperatures were designed to determine solubility under a quasi-dynamic condition inside the NMR tube. Nevertheless, as the industrial removal of H_2S from sour gas is carried out under dynamic conditions, we evaluate the dynamic selective H_2S uptake in ILs using their characteristic breakthrough curve.

2. METHODS

2.1. General Considerations. All manipulations were carried out under an anaerobic atmosphere of nitrogen using standard Schlenk and cannula techniques. The reagents and solvents were purchased from Aldrich, Merck, Acros Organics, Sigma, and Fluka and used as received. Solvents were refluxed over an appropriate drying agent, distilled, and degassed before use.

For H_2S sorption on ILs experiments, a gas mixture of H_2S/CH_4 (Praxair, 0.1% and 5.0% v/v) and carrier gases for desorption (Praxair, Ar 99.999% and O_2 99.999%) were employed.

2.2. Analytical Details. The ^{1}H and ^{13}C NMR spectra of organic compounds were recorded on a Bruker AVANCE-500 operating at 500 and 125 MHz, respectively, or on an AVANCE-300 spectrometer, operating at 300 and 75 MHz, respectively, at 298 K using $CDCl_3$ (Sigma) or D_2O (Aldrich) as solvent. Chemical shifts are reported as δ (ppm) relative to the ^{1}H and ^{13}C residues of the deuterated solvents.

2.3. Synthesis of IL. The ILs were synthesized by slight modifications of a literature procedure,[22] as follows.

2.3.1. Synthesis of [BMIM][Cl], 1. 1-methylimidazole (51.75 g; 0.63 mol) and 1-chlorobutane (70.02 g; 0.76 mol) in 20 mL of toluene were stirred at reflux for 42 h. After the removal of the volatile components, 1 was isolated as a pale-yellow viscous liquid at room temperature. Yield 120.21 g (91%). IR (KBr, cm^{-1}): (C−H) 2868; (C═C) 1632; (C═N) 1572; (C−C) 1169. ^{1}H NMR ($CDCl_3$): δ 0.88 (3H, t, C$\underline{H}_3$), 1.28 (2H, m, CH$_2$C$\underline{H}_2$CH$_3$), 1.84 (2H, m, C$\underline{H}_2$CH$_2$CH$_3$), 3.94 (3H, s, ArNC$\underline{H}_3$), 4.23 (2H, t, NC$\underline{H}_2$), 7.51 (2H, dd, NC$\underline{H}$C$\underline{H}$N), 8.86 (1H, s, NC$\underline{H}$N). ^{13}C NMR ($CDCl_3$): δ 13.07 (CH$_2$C$\underline{H}_3$); 19.03 (NC$\underline{H}_3$); 31.57 (CH$_2$C$\underline{H}_2$CH$_3$); 36.13 (C$\underline{H}_2$CH$_2$CH$_3$); 49.49 (NC$\underline{H}_2$); 122.54 (NC$\underline{H}$CHN); 123.80 (NCH$\underline{C}$HN); 136.06 (NC$\underline{H}$N).

2.3.2. Synthesis of [BMIM][Br], 2. This compound was synthesized by a procedure analogous to that described for **1** using 1-methylimidazole (11.05 g; 0.63 mol) and 1-bromobutane (62.14 g; 0.45 mol). Yield 91.01 g (92%). IR (KBr, cm^{-1}): (C−H) 2961; (C═C) 1632; (C═N) 1572; (C−C) 1169. ^{1}H NMR (D_2O): δ 0.86 (3H, t, C$\underline{H}_3$), 1.26 (2H, m, CH$_2$C$\underline{H}_2$CH$_3$), 1.79 (2H, m, C$\underline{H}_2$CH$_2$CH$_3$), 3.84 (3H, s, ArNC$\underline{H}_3$), 4.14 (2H, t, NC$\underline{H}_2$), 7.43 (2H, dd, NC$\underline{H}$C$\underline{H}$N), 8.66 (1H, s, NC$\underline{H}$N). ^{13}C NMR (D_2O): δ 12.77 (CH$_2$C$\underline{H}_3$); 18.86 (NC$\underline{H}_3$); 31.36 (CH$_2$C$\underline{H}_2$CH$_3$); 35.83 (C$\underline{H}_2$CH$_2$CH$_3$); 49.41 (NC$\underline{H}_2$); 122.60 (NC$\underline{H}$CHN); 123.60 (NCH$\underline{C}$HN); 135.91 (NC$\underline{H}$N).

2.3.3. Synthesis of [BPy][Cl], 3. This compound was synthesized by a procedure analogous to that described for **1** using pyridine (17.26 g; 0.22 mol) and 1-chlorobutane (30.33 g; 0.33 mol). Yield 50.00 g (91%). IR (KBr, cm^{-1}): (C−H) 2961; (C═C) 1639; (C═N) 1484; (C−C) 1173. ^{1}H NMR (D_2O): δ 0.85 (3H, t, C$\underline{H}_3$), 1.26 (2H, m, CH$_2$C$\underline{H}_2$CH$_3$), 1.93 (2H, m, C$\underline{H}_2$CH$_2$CH$_3$), 4.57 (2H, t, NC$\underline{H}_2$), 8.02 (2H, t,C$\underline{H}$CHN), 8.49 (1H, t, C$\underline{H}$CHCHN), 8.81 (2H, d, C$\underline{H}$NC$\underline{H}$). ^{13}C NMR (D_2O): δ 12.94 (CH$_2$C$\underline{H}_3$); 18.87 (CH$_2$C$\underline{H}_2$CH$_3$); 31.71 (C$\underline{H}_2$CH$_2$CH$_3$); 61.83 (NC$\underline{H}_2$); 128.40 (C$\underline{H}$CHN); 144.34 (C$\underline{H}$CHCHN); 145.66 (C$\underline{H}$NC$\underline{H}$).

2.3.4. Synthesis of [BPy][Br], 4. This compound was synthesized by a procedure analogous to that described for **1** using pyridine (9.08 g; 0.16 mol) and 1-bromobutane (23.68 g; 0.17 mol) in toluene (15.00 mL). Yield 33.45 g (91%). IR (KBr cm^{-1}): (C−H) 2961; (C═C) 1639; (C═N) 1484; (C−C) 1173. ^{1}H NMR (D_2O): δ 0.92 (3H, t, C$\underline{H}_3$), 1.35 (2H, m, CH$_2$C$\underline{H}_2$CH$_3$), 2.02 (2H, m, C$\underline{H}_2$CH$_2$CH$_3$), 4.69 (2H, t, NC$\underline{H}_2$), 8.15 (2H, t, C$\underline{H}$CHN), 8.62 (1H, t, C$\underline{H}$CHCHN), 8.97 (2H, d, C$\underline{H}$NC$\underline{H}$). ^{13}C NMR (D_2O): δ 13.33 (CH$_2$C$\underline{H}_3$); 19.09 (CH$_2$C$\underline{H}_2$CH$_3$); 32.94 (C$\underline{H}_2$CH$_2$CH$_3$); 61.94 (NC$\underline{H}_2$); 128.63 (C$\underline{H}$CHN); 144.54 (C$\underline{H}$CHCHN); 145.87 (C$\underline{H}$NC$\underline{H}$).

2.4. ^{1}H NMR Experiments at Different Temperatures. H_2S solubility was determined by NMR spectroscopy experiments. A sample of IL was added to a Young-Tap NMR tube containing a sealed glass capillary with D_2O. Air was evacuated under vacuum and, subsequently, the IL was exposed to a gas mixture of H_2S/CH_4 5% v/v to saturate the internal atmosphere of the NMR tube. The mixture of the acid gas flowed at a rate of 30 mL/min for 1 h at 298 K. After that the Young-Tap NMR tube was hermetically sealed and ^{1}H NMR spectra were recorded at different temperatures from 298 to 333 K, at intervals of 5 K. Before taking each spectrum at a fixed temperature, the system was allowed to reach equilibrium by keeping it under isothermal condition for a long resting period. Experiments were carried out by quintupled to get a statistical average of the integration value. The mole fraction of H_2S in IL was determined by comparing the relative intensities of the H_2S proton signal and the more acidic proton signal of the imidazolium ring in the same ^{1}H NMR spectrum (Supporting Information, S1). The chemical shifts are reported as δ (in ppm) relative to the ^{1}H residues of the *H*OD. The temperature-dependent chemical shift of the residual solvent peak (*H*OD) was corrected as stated by Gottlieb et al. and Hoffman[23−25] according to eq 1:

$$\delta = 5.051 - 0.0111T \quad (1)$$

https://doi.org/10.1021/acsomega.3c07594
ACS Omega 2024, 9, 3588−3595

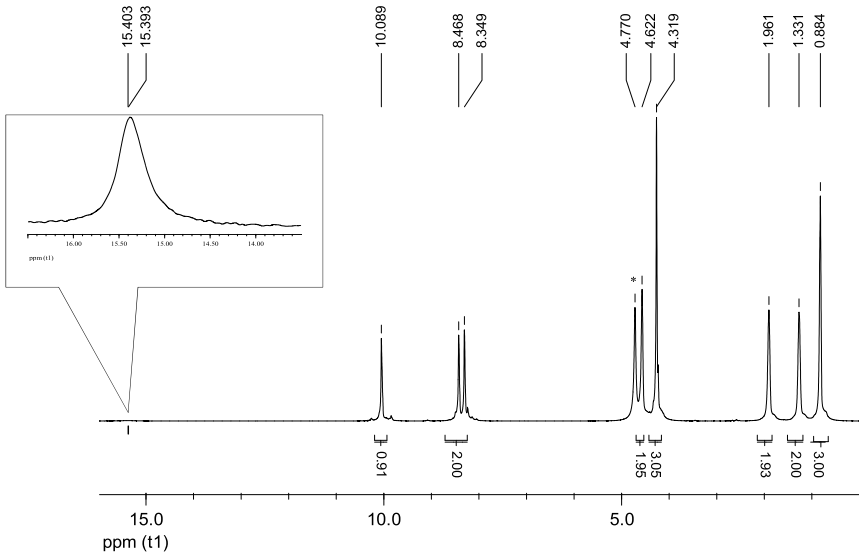

Figure 1. ^{1}H NMR at 500 MHz of [BMIM][Cl] after H_2S saturation at 298 K (* = D_2O signal).

2.5. Dynamic H_2S Experiments. Dynamic H_2S sorption experiments were carried out to evaluate the capacity of ILs for H_2S removal. Approximately 0.5 g of IL was added to the bottom of a suitable trap-like glass reactor. A gas mixture of H_2S/CH_4 with an acid concentration of 0.1% v/v was bubbled into the bottom of the liquid bed at a flow rate of 30.0 mL/min. The outlet concentration of H_2S was monitored online using an Interscan LD-17 detector. Experiments were performed until the outlet H_2S concentration equaled the starting inlet concentration. However, dilution of the outlet acid gas with air was done to extend the detector's lifetime. All experiments were kept under an isothermal condition of 298 K.

The breakthrough capacity (mg-H_2S/g-IL) was calculated by eq 2[26]:

$$BC = \frac{QMW}{wV_M} \times \left(C_o t_s - \int_0^{t_s} C(t)dt \right) \quad (2)$$

Equation 2 is readily solved by integrating the corresponding breakthrough curve obtained by plotting the outlet H_2S concentration vs time, and using the following set of variables: BC is the breakthrough capacity expressed in mg/g; Q is the total inlet flow rate (m^3/s); w is the weight of the IL introduced into the column (g); MW is the molecular weight of H_2S (34.0 mg/mmol); V_M is the molar volume of H_2S (22.4 mL/mmol); C_0 is the inlet gas H_2S concentration (ppmv); $C(t)$ is the gas outlet concentration (ppmv); dt is the saturation-exhaustion time (s).

Further details of the *BC* calculation are given in the Supporting Information (S2).

2.6. H_2S Desorption Experiment. The H_2S-contained IL was bubbled with a streaming gas (Ar or O_2) at a flow of 30.0 mL/min at room temperature (298 K) for 10 min. The outlet gas mixture was permanently online monitored. When no further H_2S was detected, the sorption experiments were repeated under the same experimental conditions until no detectable difference in H_2S removal within consecutive runs was observed.

3. RESULTS AND DISCUSSION

The ILs **1**−**4** were prepared by a procedure previously reported in the literature.[22] Analytically pure products were typically obtained in high yield (>90%). All compounds were characterized by microanalysis and IR, ^{1}H, and ^{13}C {^{1}H} NMR spectroscopy. In all cases, elemental analyses were consistent with the proposed formulation. The IR spectra of **1**−**4** possessed characteristic bands of the expected functional groups, whereas the ^{1}H and ^{13}C {^{1}H} NMR spectra of **1**−**4** are consistent with the expected structures.

The ^{1}H NMR spectrum for the saturated H_2S-[BMIM][Cl] solution showed the expected resonances for protons on the cation, with three sets of aromatic resonances rather than a significant shift in comparison to the pure IL (Figure 1). Solubilization of H_2S in [BMIM][Cl] results in a high-frequency shift (downfield) of about 1.0 ppm for resonances of the imidazolium methylene protons (−NC***H***$_2$═C***H***$_2$N−). Contrarily, the resonance of the most acidic proton (−NC***H***N−) is shifted to low frequency (high field) for about 0.3 ppm. For all resonances, loss of the splitting pattern is observed (Supporting Information, S3).

In addition, a signal assigned to the protons of H_2S dissolved in the [BMIM][Cl] appears as a broad singlet at high frequency (δ 15 ppm), likely from an N···H-SH intermolecular bond formation. It is known that the chemical shift of N−H protons can occur virtually anywhere in ^{1}H NMR spectra because the δ_H value depends on various factors such as the chemical environment of the proton in the molecular structure, solvent nature, temperature, acidity, and hydrogen intra- or intermolecular bonding. Protons interacting with nitrogen atoms may be exchangeable resulting in broad peaks. Further evidence for the assignment of the N···H-SH resonance and neglecting the possible CH_4 interactions with the IL is obtained from the HMBC (heteronuclear multiple bond coherence) experiment where no cross-peaks in the downfield region of the spectrum were observed (Supporting Information, S4).

The chemical shifts for protons of H_n-S_m species in common organic and inorganic solvents are observed at very low frequency, below δ 1 ppm.[27] However, a significant shift to higher frequency has been reported for H−S species in [N_{2224}][DMG], with the resonance of the proton on the N···H−S bond occurring at δ 6.85 ppm.[28] Other NMR experiments have been carried out and reported elsewhere to

https://doi.org/10.1021/acsomega.3c07594
ACS Omega 2024, 9, 3588−3595

determine the solubility of H_2S in different ILs. As the H_2S is in contact with the IL-containing deuterated solvents, it is not clear whether the H_2S is reacting with the mixture of the IL and the deuterated solvent, the solvent, or the IL alone. To overcome the possible interference of the solvent in this work, experiments were carried out by isolating the deuterated solvent into a closed glass capillary inset to the NMR tube.

The temperature dependence of N···H-SH proton estimated as the $\Delta\delta NH/\Delta T$ value indicates the efficacy of intermolecular hydrogen bonding. The nonhydrogen bonded N···H protons generally show a small temperature dependence of less than 3.0 ppb/K.[29,30] The value of $\Delta\delta NH/\Delta T$ found in this work for N···H-SH was 11.2 ppb/K which is much higher than 3.0 ppb/K, indicating a strong intermolecular hydrogen bonding between the acidic gas and the IL (Supporting Information, S5).

The solubility of H_2S in the IL is also highly dependent on temperature. Figure 2 shows the variation of signal intensities

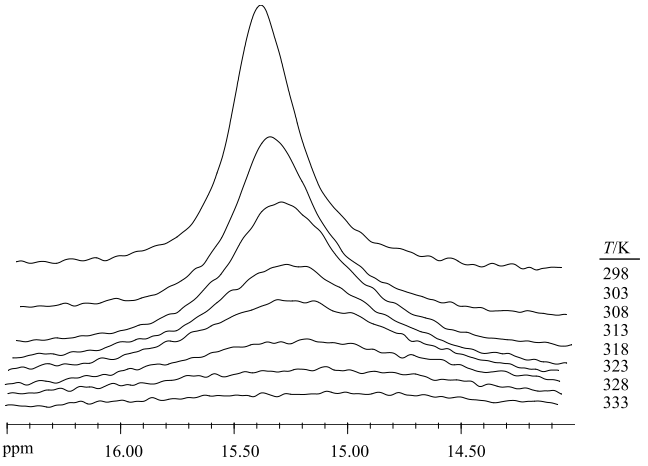

Figure 2. ^1H NMR spectra (500 MHz; D_2O) in the low-frequency region of [BMIM][Cl] after H_2S saturation at different temperatures (298−333 K).

corresponding to the N···H-SH, due to the H_2S dissolved in [BMIM][Cl], as a function of temperature. It is noteworthy that this signal decreases with increasing temperature, indicating a lower amount of H_2S dissolved in the IL at a higher temperature due to lower solubility.

To estimate the magnitude of the IL and the acid gas interaction, the level of order that takes place in the liquid/gas mixture and whether the process occurs spontaneously during H_2S dissolution in the IL, the solution standard enthalpy ($\Delta_{sol}H^o$), the solution standard entropy ($\Delta_{sol}S^o$), and the solution standard Gibbs energy ($\Delta_{sol}G^o$) were calculated by using the classical thermodynamic Van't Hoff's approach described in eqs 3−5, respectively.[31−37]

$$\left(\frac{\partial \ln X_{H_2S}}{\partial\left(\frac{1}{T}-\frac{1}{T_{hm}}\right)}\right)_p = -\frac{\Delta_{sol}H^o}{R} \tag{3}$$

$$\Delta_{sol}S^o = \frac{(\Delta_{sol}H^o - \Delta_{sol}G^o)}{T_{hm}} \tag{4}$$

$$\Delta_{sol}G^o = -RT_{hm} \times \text{Intercep} \tag{5}$$

where, R is the universal gas constant; T is the temperature; T_{hm} is the mean harmonic temperature (the use of the mean harmonic temperature in eqs 3−5 is advantageous for enthalpy−entropy compensation and separates the chemical from statistical effects).

A typical Van't Hoff plot of the H_2S solubility in [BMIM][Cl], from 298 to 333 K is displayed in Figure 3. As can be seen, the expected curve shows a straight line with a slight deviation of the linearity at higher temperatures and an acceptable determination coefficient value of 0.954.

The curve is best described by eq 6:

$$\ln X_{H2S} = 7957(T^{-1} - T_{hm}^{-1}) - 5.02 \tag{6}$$

From the slope, $\Delta_{sol}H^o$ was readily estimated according to eq 3.

Values of the Gibbs energy, enthalpy, and entropy of the acid gas dissolution process in the IL are collected in Table 1. The values of relative contributions of the thermodynamic parameter to solution processes ζ_H and ζ_{TS} are also reported. As can be seen, H_2S dissolution in [BMIM][Cl] is a spontaneous process ($\Delta_{sol}G^o < 0$). The enthalpy and entropy contributions to the gas dissolution are slightly different, with

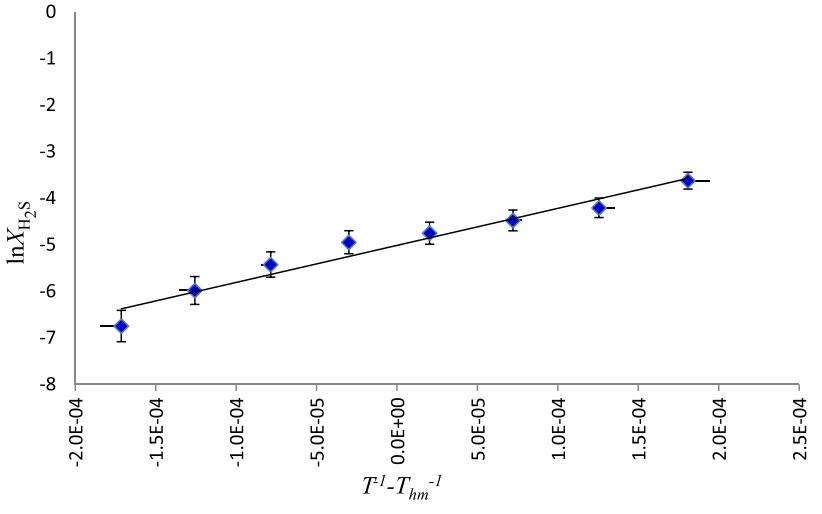

Figure 3. Van't Hoff plot for H_2S solubility in [BMIM][Cl].

https://doi.org/10.1021/acsomega.3c07594
ACS Omega 2024, 9, 3588−3595

Table 1. Apparent Thermodynamic Solution Functions of H_2S/CH_4 in [BMIM][Cl]

$\Delta_{sol}H^o$ (kJmol^{-1})	$\Delta_{sol}G^o$ (kJmol^{-1})	$\Delta_{sol}S^o$ (JK^{-1} mol^{-1})	ζ_H [a]	ζ_{TS} [b]
−66.15	−13.14	−168.19	0.55	0.45

[a] $\zeta_H = \frac{|\Delta H^o|}{|\Delta H^o| + |T\Delta S^o|}$. [b] $\zeta_{TS} = \frac{|T\Delta S^o|}{|\Delta H^o| + |T\Delta S^o|}$.

enthalpy just overcoming the entropy loss (ζ_H = 55% and ζ_H = 45%). $\Delta_{sol}H^o$ is exothermic ($\Delta_{sol}H^o < 0$), which explains the decreasing solubility of H_2S in [BMIM][Cl] with increasing temperature.

The gas solubility enthalpy indicates an exothermic gas−liquid physisorption, where no formal chemical bond between [BMIM][Cl] and H_2S is generated. The negative enthalpy value may arise from cavity formation and the strong solute−solvent interactions, as revealed by the ^{1}H NMR spectral evidence. Because of the strong N···H-SH association, the local entropy diminishes due to the partial immobilization of the gas into the ionic solvent.

The magnitude of the enthalpy amounts to a fifth of the H−S bond energy, which means there is no possible H−S bond activation during the gas sorption process mediated by the IL.

Values of the in-solution thermodynamic functions are close to those found for the highly efficient absorbents for H_2S absorption based on multiple Lewis base functionalized protic ILs (MLB-PILs) solutions of [TMDAPH][Ac], [PMDPTAH]-[Ac], and [TDMAPAH][Ac].[11]

Following the fact of the spontaneous H_2S sorption on [BMIM][Cl] and its readily thermal desorption, we step forward to investigate the H_2S breakthrough capacity of four different ILs under bench dynamic conditions. Data from experiments of dynamic sorption capacity expressed as the mass fraction of H_2S retained in the liquid phase are useful to set parameters for the scale-up process when a dimensional approach is used.

The H_2S dynamic sorption profiles as a function of time are shown in Figure 4. For all the ILs, the breakthrough curves presented a typical S-shape line. Initially, the IL retains selectively the H_2S from the gas mixture and the evolved gas resulting in a steady zone of the curve near zero. As the gas mixture is bubbling out into the liquid phase, a homogeneous mass transfer zone is established, resulting in an efficient H_2S retainer liquid bed. A breaking point, the breakthrough, is reached when a fast change in the slope occurs. After that, the curve sharply increases to a saturation level where the H_2S outlet concentration equals the inlet concentration ($C_{0,H2S}$) at the equilibration time, the time at which the entire bed is in equilibrium with the feed.

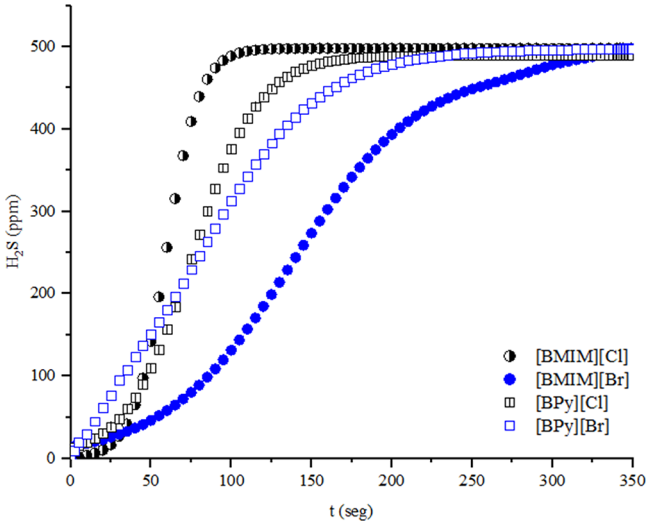

Figure 4. Breakthrough curves of H_2S intake for different ILs at 298 K.

The difference between breakthrough and equilibration times depends on the mass transfer rate. In Figure 4, it can be seen that [BMIM][Cl] has a higher mass transfer rate. The breakthrough curve is almost a vertical line. Meanwhile, the curves for [BPy][Cl] and [BPy][Br] show intermediate mass transfer rates between those of [BMIM][Cl] and [BMIM][Br]. In this case, the increase in H_2S concentration in the effluent after the initial breakthrough is steeper because the ILs are performed more efficiently than [BMIM][Cl].

On the other hand, the breakthrough curve for [BMIM][Br] approaches a symmetrical S-shape, which would be the ideal case for the sorption process, with a flat mass transfer front. These features resulted in the most efficient system for H_2S removal.

The saturation time increases in the order [BMIM][Cl] < [BPy][Cl] = [BPy][Br] < [BMIM][Br] with breakthrough capacity ranging between 0.16 and 0.38 mg/g.

Ideally, for an upscaling industrial process, a system that generates a breakthrough curve with a symmetrical S-shape with a flat mass transfer front is desirable. The breakthrough time for this ideal process, which occurs at the midpoint of the real S-shaped breakthrough curve, is known as the stoichiometric time. Its variables allow us to determine practical and operational parameters for an industrial process.

The difference in the IL breakthrough capacity is rather interesting. For ILs based on BPy, the effect of the anion on the sorption capacity is not apparent, whereas in those based on BMIM, anions seem to determine largely their sorption capacity. These results seem more likely due to the effect of cation−anion association in each case, which would determine the H_2S−solvent interaction.

The enthalpy value of the solution process suggests that [BMIM][Br] can be efficiently regenerated at a low-energy cost (atmospheric pressure and room temperature) to be further reused for the same purpose. The recyclability of ILs was studied by using consecutive H_2S sorption−desorption cycles. While sorption experiments consist of bubbling the H_2S/CH_4 gas mixture into the IL until saturation, desorption consists of bubbling air or Argon into the liquid for some time at 298 K, usually for 10 min. Figure 5 resumes the efficiency (%) and total removed H_2S vs cycle. From Figure 5, it is clear that [BMIM][Br] could be reused 10 times before losing less than 9% of its H_2S removal efficiency at a rate of less than 1.0% per cycle. From the linear decay tendency of the H_2S removal efficiency, the mass of H_2S removed witting cycles of sorption−desorption until reaching 50% of ILs efficiency, amounts to 16.20 mg/g, which is equivalent to a loading or solubility of 0.11 mol/mol at 298 K and 1.0 bar.

Although the total H_2S removal capacity of [BMIM][Br] is in the range for alkanol amine and a mixture of the alkanol amine solutions technology (0.1−1.0 mol/mol),[38] it is rather lower for the task-specific IL for acid gas absorption. For instance, $[N_{2224}]_2$[maleate] has shown an H_2S solubility of 1.43 mol/mol.[38] However, a direct comparison of recyclability with literature values is rather difficult due to the different

https://doi.org/10.1021/acsomega.3c07594
ACS Omega 2024, 9, 3588−3595

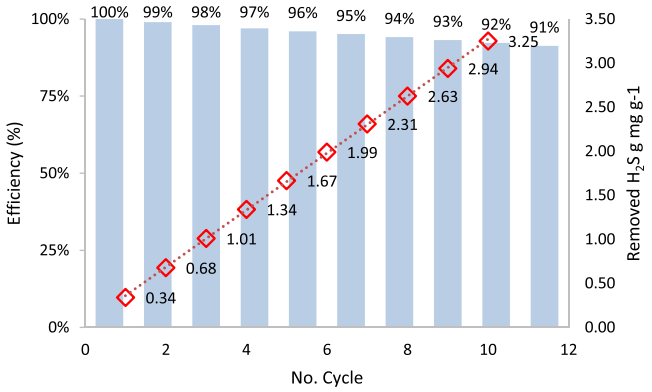

Figure 5. H_2S removal efficiency with [BMIM][Br] in consecutive cycles of sorption−desorption experiments.

experimental settings and approaches used. Given the fact that [BMIM][Br] should be considered as a physical absorbent, it is unlikely to replace alkanolamines for acid gas removal.

4. CONCLUSIONS

In this work, ^{1}H NMR spectroscopy was employed to determine the solubility of H_2S in [BMIM][Cl] at different temperatures. Experiments were carefully carried out to eliminate the possibility of H_2S−deuterated solvent interactions. From the results, the thermodynamic solution parameters of H_2S in [BMIM][Cl] were estimated. The results indicated that the solubility of H_2S in [BMIM][Cl] is an exothermic gas−liquid physisorption with an enthalpy value of −66.15 KJ mol^{-1}. ^{1}H NMR spectra of the H_2S dissolved in [BMIM][Cl] showed a large chemical shift to low frequencies of the H−S signal, which is in good concordance with the negative enthalpy value. These results indicate strong solute−solvent interactions most probably as a result of a strong S−H association with the ILs anion. Partial immobilization of the H_2S molecules into the ionic solvent is also attributed to lower local entropy. Although strong interaction between H_2S and the IL is evident from ^{1}H NMR experiments, no H−S bond activation is achieved since the magnitude of the enthalpy is significantly lower than the H−S bond energy.

Results from dynamic experiments using representative operating conditions of sour gas "sweetening" are in great agreement with NMR results. Solubility seems to be conditioned by the nature of the anion. Regenerability of the IL is readily afforded by bubbling it with a stream inert gas at 298 K. After 50 cycles of gas sorption−desorption into [BMIM][Br], it is removed up to 16.20 mg/g. Since ILs advantage amine solution technology in their low volatility and chemical stability, ILs remain a promising alternative in upgrading sour gas.

Although the dynamic approach is rather useful in determining the amount of H_2S retained in the IL bed on a realistic experimental setting results demonstrate that ^{1}H NMR experiments are precise, exact, robust, and useful for both the quantitative determination of the dissolved acid gas in the IL as for gaining a better understanding of the interaction between H_2S and IL.

■ ASSOCIATED CONTENT

Supporting Information

The Supporting Information is available free of charge at https://pubs.acs.org/doi/10.1021/acsomega.3c07594.

Further details for the calculation of the mole fraction of H_2S in the ionic liquids, calculation of the harmonic mean temperature, calculation of the breakthrough capacity and calculation of the temperature dependence of N···H-SH proton. ^{1}H NMR spectrum of [BMIM][Cl] and [BMIM][Cl] saturated with H_2S/CH_4 and, HMBC NMR spectrum of the [BMIM][Cl] saturated with H_2S/CH_4 (PDF)

■ AUTHOR INFORMATION

Corresponding Authors

Jeannette Zárraga − *Grupo de Energía y Procesos Sustentables, Instituto de Ciencias Aplicadas, Facultad de Ingeniería, Universidad Autónoma de Chile, Santiago 8200000, Chile*; Email: jeannette.zarraga@uautonoma.cl

Juan Chirinos − *Grupo de Energía y Procesos Sustentables, Instituto de Ciencias Aplicadas, Facultad de Ingeniería, Universidad Autónoma de Chile, Santiago 8200000, Chile*; orcid.org/0000-0002-1547-4036; Email: juan.chirinos@uautonoma.cl

Authors

Mariana Zapata − *Laboratorio de Polímeros, Departamento de Química, Facultad Experimental de Ciencias and Instituo de Superficies y Catálisis, Facultad de Ingeniería, Universidad del Zulia, Maracaibo 4001A, Venezuela*

Darmenia Ibarra − *Laboratorio de Polímeros, Departamento de Química, Facultad Experimental de Ciencias, Universidad del Zulia, Maracaibo 4001A, Venezuela*

Darlin Duarte − *Laboratorio de Polímeros, Departamento de Química, Facultad Experimental de Ciencias, Universidad del Zulia, Maracaibo 4001A, Venezuela*

Ángel Morillo − *Laboratorio de Polímeros, Departamento de Química, Facultad Experimental de Ciencias, Universidad del Zulia, Maracaibo 4001A, Venezuela*

Ligia Llovera − *Instituto Venezolano de Investigaciones Científicas, Caracas 1020, Venezuela*

Eduardo Gonzalez − *Facultad de Ciencias de la Salud, Universidad Católica de Santa Fe, S3000 Santa Fe de la Vera Cruz, Santa Fe, Argentina*

Victor Ferrer − *Unidad de Desarrollo Tecnológico, Universidad de Concepción, Coronel 4191996, Chile; Centro Nacional de Excelencia para la Industria de la Madera (CENAMAD), Pontificia Universidad Católica de Chile, Santiago 7820436, Chile*

Complete contact information is available at: https://pubs.acs.org/10.1021/acsomega.3c07594

Notes

The authors declare no competing financial interest.

■ ACKNOWLEDGMENTS

M.Z. gratefully acknowledges ANTARES I&D for financial support. Co-authors from Universidad del Zulia deeply acknowledge the support of Instituto de Superficies y Catálisis-Universidad del Zulia. V.F. gratefully acknowledges ANID BASAL FB 210015 for financial support.

■ REFERENCES

(1) Georgiadis, A.G.; Charisiou, N.D.; Goula, M.A. Removal of Hydrogen Sulfide From Various Industrial Gases: A Review of The Most Promising Adsorbing Materials. *Catalysts* **2020**, *10*, 521.

(2) Morris, J. Method and system for removing hydrogen sulfide from sour oil and sour water, EP 2 770 041 A1, 2014.
(3) Rubright, S.L.M.; Pearce, L.L.; Peterson, J. Environmental Toxicology of Hydrogen Sulfide. *Nitric Oxide* **2017**, *71*, 1−13, DOI: 10.1016/j.niox.2017.09.011.
(4) Bui, M.; Adjiman, C. S.; Bardow, A.; Anthony, E. J.; Boston, A.; Brown, S.; Fennell, P. S.; Fuss, S.; Galindo, A.; Hackett, L. A.; Hallett, J. P.; Herzog, H. J.; Jackson, G.; Kemper, J.; Krevor, S.; Maitland, G. C.; Matuszewski, M.; Metcalfe, I. S.; Petit, C.; Puxty, G.; Reimer, J.; Reiner, D. M.; Rubin, E. S.; Scott, S. A.; Shah, N.; Smit, B.; Trusler, J. P. M.; Webley, P.; Wilcox, J.; Mac Dowell, N. Carbon capture and storage (CCS): The way forward. *Energy Environ. Sci.* **2018**, *11*, 1062−1176.
(5) MacDowell, N.; Florin, N.; Buchard, A.; Hallett, J.; Galindo, A.; Jackson, G.; Adjiman, C. S.; Williams, C. K.; Shah, N.; Fennell, P. An overview of CO2 capture technologies. *Energy Environ. Sci.* **2010**, *3*, 1645−1669.
(6) Sassi, M.; Gupta, A. K. A. *Sulfur Recovery from Acid Gas Using the Claus Process and High-Temperature Air Combustion (HiTAC) Technology*; 2016.
(7) Ibrahim, A. Y.; Ashour, F. H.; Gadalla, M. A. Heliyon Exergy study of amine regeneration unit using diethanolamine in a refinery plant: A real start-up plant. *Heliyon.* **2021**, *7*, No. e06241.
(8) Shoukat, U.; Pinto, D. D. D.; Knuutila, H. K. Study of Various Aqueous and Non-Aqueous Amine Blends for Hydrogen Sulfide Removal from Natural Gas. *Processes* **2019**, *7*, 160 DOI: 10.3390/pr7030160.
(9) Fedich, R.B.; Kortunov, P.; Siskin, M.; WO2013/138437 A2, 2013.
(10) Zhang, X.; Xiong, W.; Shi, M.; Wu, Y.; Hu, X. Task-specific ionic liquids as absorbents and catalysts for efficient capture and conversion of H2S into value-added mercaptan acids. *Chem. Eng. J.* **2021**, *408*, No. 127866.
(11) Zheng, W.; Wu, D.; Feng, X.; Hu, J.; Zhang, F.; Wu, Y. T.; Hu, X. B. Low viscous Protic ionic liquids functionalized with multiple Lewis Base for highly efficient capture of H2S. *J. Mol. Liq.* **2018**, *263*, 209−217.
(12) Hospital-Benito, D.; Hallett, J. P.; Palomar, J.; Lemus, J.; Santiago, R.; Welton, T. Process Analysis of Ionic Liquid-Based Blends as H2S Absorbents: Search for Thermodynamic/Kinetic Synergies. *ACS Sustainable Chem. Eng.* **2021**, *9*, 2080 DOI: 10.1021/acssuschemeng.0c07229.
(13) Li, F.; Laaksonen, A.; Zhang, X.; Ji, X. Rotten Eggs Revaluated: Ionic Liquids and Deep Eutectic Solvents for Removal and Utilization of Hydrogen Sulfide. *Ind. Eng. Chem. Res.* **2022**, *61*, 2643 DOI: 10.1021/acs.iecr.1c04142.
(14) Welton, T. Ionic liquids: a brief history. *Biophys. Rev.* **2018**, *10*, 691−706, DOI: 10.1007/s12551-018-0419-2.
(15) Lima, E. C.; Gomes, A. A.; Nguyen, H. Comparison of the nonlinear and linear forms of the van't Hoff equation for calculation of adsorption thermodynamic parameters (ΔS° and ΔH°). *J. Mol. Liq.* **2020**, *311*, No. 113315.
(16) Canuto, A.V.S.; Echevarria, A.; et al. 1H NMR for quantifying sulfide trapping efficiency by using 1,3,5-tris(2-hydroxyethyl)-1,3,5-triazinane. *Magn. Reson. Chem.* **2014**, *52*, 353−357, DOI: 10.1002/mrc.4072.
(17) Bailey, T.S.; Zakharov, L.N.; Pluth, M.D. Understanding Hydrogen Sulfide Storage: Probing Conditions for Sulfide Release from Hydrodisulfides. *J. Am. Chem. Soc.* **2014**, *136*, 10573−10576, DOI: 10.1021/ja505371z.
(18) Mousavi, S. P.; Kohani, R. N.; Atashrouz, S.; Hadavimoghaddam, F.; Abedi, A.; Sarapardeh, A. H.; Mohaddespour, A. Modeling of H 2 S solubility in ionic liquids: comparison of white - box machine learning, deep learning and ensemble learning approaches. *Sci. Rep.* **2023**, *13*, 7946.
(19) Shokouhi, M.; Adibi, M.; Jalili, A.H.; Hosseini-jenab, M.; Mehdizadeh, A. Solubility and Diffusion of H2S and CO2 in the Ionic Liquid 1-(2-Hydroxyethyl)-3-methylimidazolium Tetrafluoroborate. *J. Chem. Eng. Data* **2010**, *87*, 1663−1668, DOI: 10.1021/je900716q.
(20) Abdi, J.; Hadipoor, M.; Hamid, S.; Faraj, E.; Vaferi, B. OPEN A modelling approach for estimating hydrogen sulfide solubility in fifteen different imidazole - based ionic liquids. *Sci. Rep.* **2022**, *12*, 4415.
(21) Thermodynamics, J. C.; Jalili, A. H.; Mehdizadeh, A.; Shokouhi, M.; Ahmadi, A. N.; Hosseini-Jenab, M.; Fateminassab, F. Solubility and diffusion of CO2 and H2S in the ionic liquid 1-ethyl-3-methylimidazolium ethylsulfate. *J. Chem. Thermodyn.* **2010**, *42*, 1298−1303.
(22) Huddleston, J. G.; Visser, A. E.; Reichert, W. M.; Willauer, H. D.; Broker, G. A.; Rogers, R. D. Characterization and comparison of hydrophilic and hydrophobic room temperature ionic liquids incorporating the imidazolium cation. *Green Chem.* **2001**, *3*, 156−164.
(23) Gottlieb, H. E.; Kotlyar, V.; Nudelman, A. NMR chemical shifts of common laboratory solvents as trace impurities. *J. Org. Chem.* **1997**, *62*, 7512−7515.
(24) Fulmer, G. R.; Miller, A. J. M.; Sherden, N. H.; Gottlieb, H. E.; Nudelman, A.; Stoltz, B. M.; Bercaw, J. E.; Goldberg, K. I. NMR chemical shifts of trace impurities: Common laboratory solvents, organics, and gases in deuterated solvents relevant to the organometallic chemist. *Organometallics.* **2010**, *29*, 2176−2179.
(25) Hoffman, R. E. Standardization of chemical shifts of TMS and solvent signals in NMR solvents. *Magn. Reson. Chem.* **2006**, *44*, 606−616.
(26) Ros, A.; Montes-moran, M. A.; Fuente, E.; Nevskaia, D. M. Dried Sludges and Sludge-Based Chars for H2S Removal at Low Temperature: Influence of Sewage Sludge Characteristics. *Environ. Sci. Technol.* **2006**, *40*, 302−309.
(27) Hynes, J. B.; Muller, E. Nuclear Magnetic Resonance of Hydrogen Polysulfides in Molten Sulfur. *J. Phys. Chem.* **1966**, *7*, 3733−3735.
(28) Huang, K.; Cai, D. N.; Le Chen, Y.; Wu, Y. T.; Hu, X. B.; Zhang, Z. B. Dual Lewis base functionalization of ionic liquids for highly efficient and selective capture of H2S. *ChemPlusChem* **2014**, *79*, 241−249.
(29) Crisp, G.T.; Jiang, Y. Intramolecular hydrogen bonding of (+)-biotin and biotin derivatives in organic solvents. *Arkivoc* **2001**, *2001*, 77−87, DOI: 10.3998/ARK.5550190.0002.707.
(30) Gellman, S. H.; Dado, G. P.; Liang, G. B.; Adams, B. R. Conformation-Directing Effects of a Single Intramolecular Amide-Amide Hydrogen Bond: Variable-Temperature NMR and IR Studies on a Homologous Diamide Series. *J. Am. Chem. Soc.* **1991**, *113*, 1164−1173.
(31) Long, B.; Li, J.; Song, Y.; Du, J. Temperature Dependent Solubility of α-Form L-Glutamic Acid in Selected Organic Solvents: Measurements and Thermodynamic Modeling. *Ind. Eng. Chem. Res.* **2011**, 8354−8360, DOI: 10.1021/ie200351b.
(32) Zhang, X.; Gobas, F. A. P. C. A Thermodynamic analysis of the relationships between molecular size, hydrophobicity, aqueous solubility and octanol-water partitioning of organic chemicals. *Chemosphere.* **1995**, *31*, 3501−3521.
(33) Tao, M.; Wang, Z.; Gong, J.; Hao, H.; Wang, J. Determination of the Solubility, Dissolution Enthalpy, and Entropy of Pioglitazone Hydrochloride (Form II) in Different Pure Solvents. *Ind. Eng. Chem. Res.* **2013**, *52*, 3036 DOI: 10.1021/ie303588j.
(34) Delgado, D. R.; Rodríguez, G. A.; Martínez, F. Thermodynamic study of the solubility of sulfapyridine in some ethanol + water mixtures. *J. Mol. Liq.* **2013**, *177*, 156−161.
(35) Chen, J.; Nan, G.; Yang, R.; Zhang, S.; Bian, X.; Yang, G. Solubility of three types of benzamide derivatives in toluene, ethyl acetate, acetone, chloroform, methanol, and water at temperatures ranging from 288. 15 to 328. 15 K at atmospheric pressure. *J. Mol. Liq.* **2015**, *204*, 137−146.
(36) Fathi-azarbayjani, A.; Abbasi, M.; Vaez-gharamaleki, J.; Jouyban, A. Measurement and correlation of deferiprone solubility: Investigation of solubility parameter and application of van't Hoff equation and Jouyban − Acree model. *J. Mol. Liq.* **2016**, *215*, 339−344.

(37) Zhao, T.; Li, P.; Feng, X.; Hu, X.; Wu, Y. Study on absorption and spectral properties of H2S in carboxylate protic ionic liquids with low viscosity. *J. Mol. Liq.* **2018**, *266*, 806−813.
(38) Pudi, A.; Rezaei, M.; Signorini, V.; Andersson, M. P.; Baschetti, M. G.; Mansouri, S. S. Hydrogen sulfide capture and removal technologies: A comprehensive review of recent developments and emerging trends. *Sep. Purif. Technol.* **2022**, *298*, No. 121448.

https://doi.org/10.1021/acsomega.3c07594
ACS Omega 2024, 9, 3588−3595